A MICROMACHINED QUARTZ AND STEEL PRESSURE SENSOR OPERATING UPTO 1000ºC AND 2000 TORR

Scott A. Wright and Yogesh B. Gianchandani
Engineering Research Center for Wireless Integrated MicroSystems (WIMS)
University of Michigan, Ann Arbor, MI, USA

ABSTRACT

This paper describes microdischarge-based pressure sensors which operate by measuring the change, with pressure, in the spatial current distribution of pulsed DC microdischarges. These devices are well-suited for high temperature operation because of the inherently high temperatures of the ions and electrons in the microdischarges, and are designed to allow for unequal expansion of electrodes and substrate during high temperature operation. These sensors use three-dimensional arrays of horizontal bulk metal electrodes embedded in quartz substrates with electrode diameters of 1-2 mm and 50-100 μm inter-electrode spacing. The sensors were operated in nitrogen over a range of 10-2,000 Torr, at temperatures as high as 1,000˚C. The maximum measured sensitivity was 5,420 ppm/Torr at the low end of the dynamic range and 500 ppm/Torr at the high end, while the temperature coefficient of sensitivity ranged from -925 ppm/K to -550 ppm/K.

INTRODUCTION

High temperature pressure sensors have uses in numerous industrial sectors, and have been used in gas turbine engines, coal boilers, furnaces, and machinery for oil/gas exploration. A variety of microscale solutions have been explored. Fabry-Perot, and other interferometers, have been used on the ends of fiber optic cables and have been operated at temperatures of 800˚C using sapphire membranes [1]. Another sensing technology uses Bragg gratings, which are photo inscribed into fibers, and used to trace wavelength shifts caused by pressure and temperature changes at temperatures exceeding 350˚C, and potentially over 1,500˚C [2]. Piezoresisitve pressure sensors with diaphragms made from silicon carbide [3], and more recently even Si [4], have been reported to operate at 600ºC. Sapphire membranes have also been used in this context [5].

Microdischarges, or microplasmas, are miniature plasmas created in gases between electrodes and are used for on-chip chemical sensing and other applications. Devices utilizing microdischarges are well suited for high temperature operation as the electrons have average thermal energies exceeding 3 eV (34,815 K) [6] away from the cathode. Ions have thermal energies exceeding 0.03 eV (621 K) in a 23ºC (296 K) ambient environment.

These microdischarge-based pressure sensors operate by measuring the change in spatial current distribution of microdischarges with pressure. The targeted pressure range is 10-2,000 Torr, as might be encountered in a variety of manufacturing applications. As gas pressure increases, the mean free path of ionized molecules is reduced and consequently, the breakdown and discharge characteristics are altered. Microdischarge-based pressure sensors are fundamentally different than ion gauges, which are not effective at atmospheric pressure because the small mean free path of the created ions, 20-65 nm, makes them difficult to detect at the collector [7].

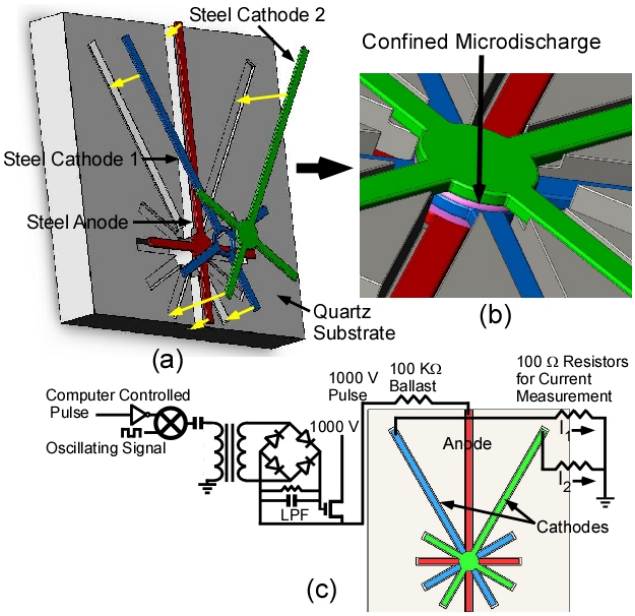

Figure 1: *Schematic of (a) stainless steel electrodes above quartz chip, illustrating electrode placement, (b) microdischarge chamber during operation, and (c) pulse generating, isolation, and readout circuitry used for sensor operation.*

A planar thin-film version of the microdischarge-based pressure sensor was first reported in [8], and operated at temperatures upto 200˚C, while this paper expands upon [9].

This paper describes a microdischarge-based microscale pressure sensor geometry that uses bulk foils in a two-cathode stack in a quartz substrate. In this effort, we explore the use of multiple cathodes. Multiple anodes may also be used; however, anode current shows excessive pressure dependence because of the high mobility of electrons that dominate it [10]. This high sensitivity results in relatively small dynamic ranges, thereby limiting the utility of multi-anode configurations. While this effort focuses on the performance of these devices in a nitrogen ambient, with appropriate encapsulation, they may be used in corrosive or liquid ambients.

DEVICE DESIGN AND OPERATION

The pressure sensor structure consists of several electrodes suspended over a cavity in a quartz chip (Fig. 1). Each electrode has a single lead for electrical contact and between one and three additional supports, which maintain the suspended position of the electrode. A microdischarge chamber exists in the center of the chip, in a through-hole, as shown in Fig. 1(b). A single disk-shaped anode electrode serves as the bottom of the

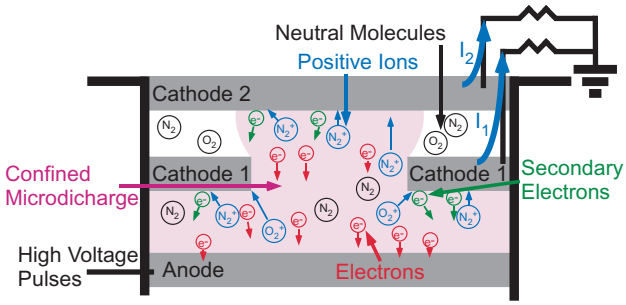

Figure 2: *Theoretical diagram of a microdischarge between a single anode and two cathodes in a microdischarge chamber. Changes in the ion distribution vary the currents in the cathodes.*

chamber while the center electrode is torus-shaped, allowing the discharges to exist between the bottom anode and both cathodes. The top cathode is disk-shaped as well, confining the discharges.

To determine the pressure, it is first necessary to separately determine the current in two of the cathodes. These current components are denoted as I_1 in the proximal cathode (cathode 1) and I_2 in the distal cathode (cathode 2). The differential current, expressed as a fraction of the total peak current, $(I_1 - I_2) / (I_1 + I_2)$, is treated as the sensor output. At low pressures, current favors the farthest cathodes, while at high pressures, the opposite occurs. An important benefit of using a differential output that is expressed as a fraction of the total is that the exact magnitudes are less important than fractional changes.

To control power consumption and parasitic heating in the pressure sensors, pulsed DC microdischarges are used, as opposed to constant DC discharges. A computer controlled, single ended, transformer coupled, gate drive circuit creates the pulses (Fig. 1(c)). A current limiting ballast resistor is used in series with the anode, and 100-Ω resistors are used in series with each cathode to measure current.

The basic operation of a DC microdischarge in a sensor is illustrated in Fig. 2, indicating electron and ion transport. The electrons are drawn towards the anode, whereas the positive ions are drawn to the two separate cathodes forming positively charged sheaths around them. Upon cathode impact, the energetic ions eject high energy secondary electrons from the cathodes, which sustain the microdischarges by ionizing additional neutral molecules and continuing the breakdown process. The current in each cathode is composed of a combination of positive ions impacting the cathodes from the microdischarges and secondary electrons ejected from the cathodes upon ion impact. Further away from the cathodes, the current is carried primarily by the faster moving electrons, which cannot reach the cathodes because of surrounding sheaths.

Sensor characteristics such as the sensitivity, pressure dynamic range, and temperature dynamic range depend on a variety of dimensional parameters, including inter-electrode spacing, electrode diameter, and the cathode thickness. (Cathode thickness effects sheath sizes as well as electrode spacing). The anode/cathode spacing in these sensors is set to produce measurable results up to 1,000ºC. (The sensors are designed to function with an applied voltage of 1,000 V; altering the voltage results in different sensitivities.) A typical sensor design with electrodes spaced 50 µm apart, 1-2 mm in diameter, and 125 µm thick is shown in Fig. 3. These sensors have active areas of 0.8-3 mm^2 and are fabricated on 1 cm^2 chips.

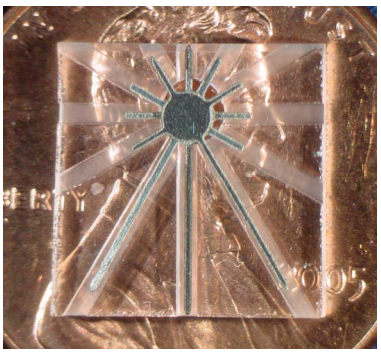

Figure 3: *Pressure sensor with electrodes spaced 50 µm apart and 125 µm in thickness on a U.S. penny.*

FABRICATION

A fabrication method that accommodates the expansion mismatch between electrodes and substrate is used (Fig. 4). For the electrodes, #302 stainless steel is used for several reasons. Primarily, it is robust, inexpensive, easily machinable by micro-electro-discharge machining and photochemical etching, and has a sufficient secondary emission coefficient (i.e. 0.02 secondary electrons per incident ion in a nitrogen ambient). Additionally, it is oxidation-resistant at high temperatures and can be heated to 1,420ºC before melting. Alternate refractory metals such as tungsten, molybdenum, and niobium oxidize at high temperatures in air, making them less desirable. Platinum, iridium, and platinum-rhodium are attractive options but are significantly more expensive than stainless steel.

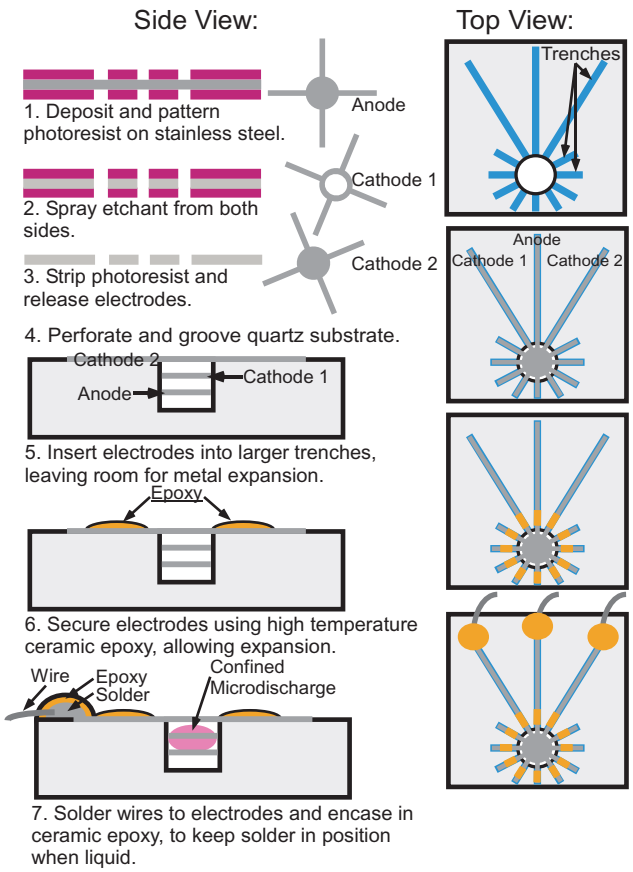

Figure 4: *Top and side view of the fabrication process.*

The electrodes are lithographically patterned and etched from stainless steel foil, using photochemical machining. This process involves coating a thin sheet of metal with photoresist, exposing the resist, and spraying the sheet with a chemical etchant to dissolve the exposed metal. The exposed metal is completely removed, leaving through-holes in the sheet, and the resist is stripped (Fotofab, Chicago IL).

Next, the electrodes are integrated into the substrate. An arrangement that accommodates the expansion mismatch between electrodes and substrate is necessary. Trenches of specified depths and a through-hole in the center are cut into a quartz chip. Both mechanical and wet-etch processes can be used for this purpose. The electrodes are assembled into the trenches, and the circular electrodes are placed in the through-hole. The different depths between the various trenches specify the discharge gap spacing, as the electrodes lie flush with the bottom of the trenches. Ceramic epoxy holds the electrode lead and support arms in place, without adhering to the stainless steel. This allows the leads and supports to expand separately from the quartz chip and the ceramic epoxy without buckling. High temperature-compatible wires are soldered to the electrodes and the solder is encased in ceramic. This ceramic keeps the solder in position so it maintains electrical contact, even at high temperatures.

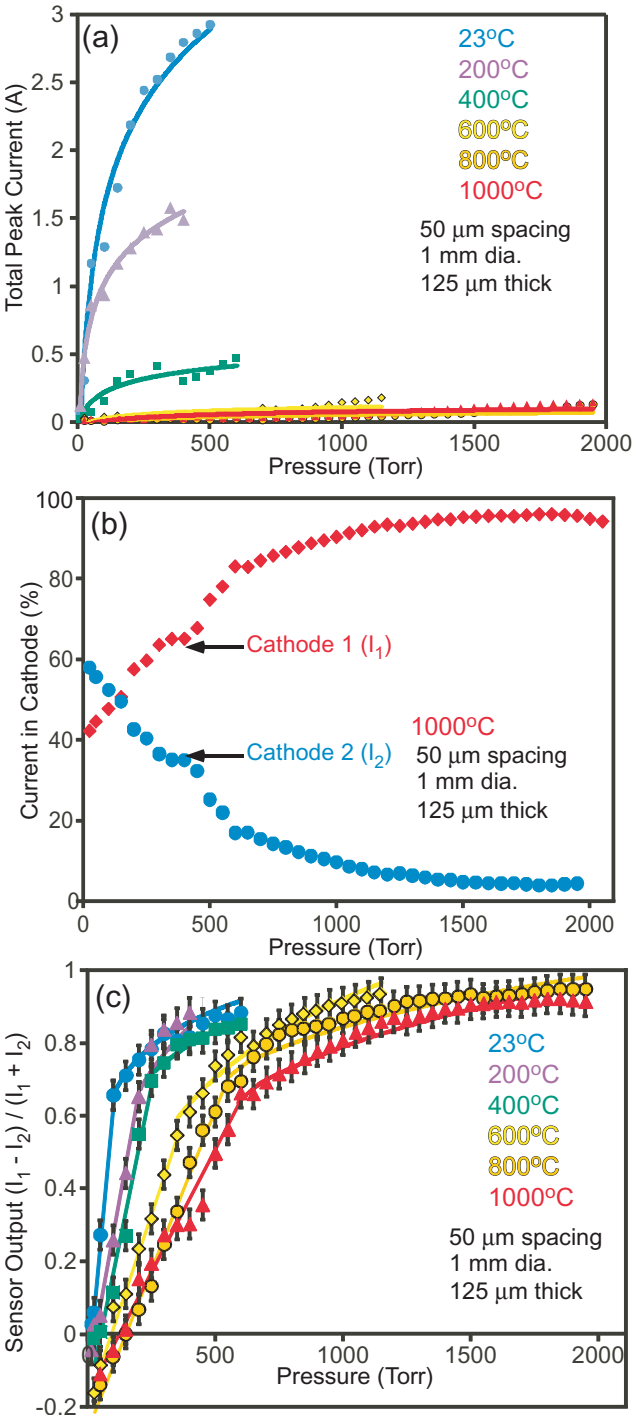

Figure 5: *Sensor output as a function of pressure in sensors with electrodes spaced 50 µm apart, 1 mm in diameter, and 125 µm thick. (a) Sum of the pulse currents in two cathodes as a function of pressure and temperature. The empirical curves for each temperature are indicated by the solid lines. (b) Percentage of total current in the cathodes at 1,000˚C. (c) Differential current output determined from the percentage of total current. Each data point is the average of 100 measurements. The two empirical curves per temperature are indicated by the solid lines.*

RESULTS AND DISCUSSION

Pressure sensors were fabricated and tested at various temperatures upto 1,000ºC, measuring pressures between 10 Torr and 2,000 Torr. Pulses, 1-20 ms in duration, were applied at a rate of 2-10 Hz to the anodes of the sensors with positive voltages between 700 V and 1,000 V. The pulses consumed between 168 µJ and 6 mJ each.

The applied voltage pulses resulted in current pulses through each cathode. The transient current peaks were approximately 50-200 ns in duration, with amplitudes of 1.3 mA to 2.85 A, varying with temperature and pressure. The sum of the measured cathode current peaks for a device is presented in Fig. 5(a). At each temperature, this sum conforms to the equation:

$$I_{pk1} + I_{pk2} = C_1 \cdot \ln(p) - C_2 \qquad (1)$$

The terms C_1 and C_2, determined by a least-squares fit to the measured data.

The sensors were tested in a nitrogen chamber with temperature and pressure control. Figure 5(b) shows fractional cathode currents, at 1,000˚C, for a sensor with electrodes that were spaced 50 µm apart, 1 mm in diameter, and 125 µm thick. As noted, the output of the sensor is the differential peak current between two cathodes, expressed as a fraction of the total peak current.

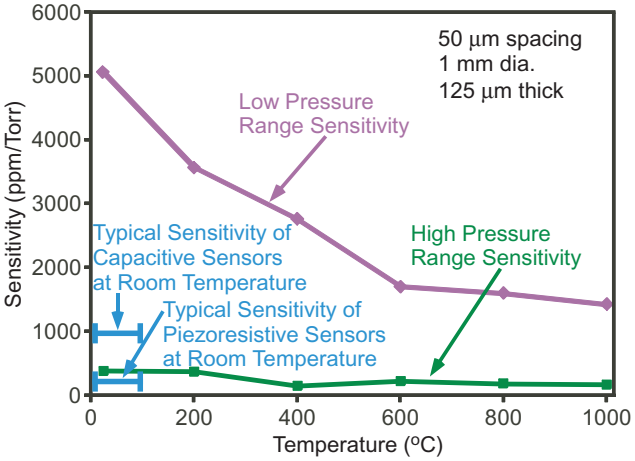

Figure 6: *The average sensitivities in both the low and high pressure ranges for the sensor in Fig. 5 as functions of temperature.*

This is shown in Figure 5(c). The sensors demonstrate two regions of sensitivity (similar in some sense to touch-mode capacitive pressure sensors [11]). At low pressures the response is highly linear, whereas at high pressures it conforms to equation 1. The transition between these two regions rises from about 100 Torr at room temperature to about 500 Torr at 1,000°C.

The average sensitivities in the low pressure and high pressure operating regions of this sensor are shown in Fig. 6 as functions of temperature. One sensor design typically demonstrated the maximum lower pressure sensitivity, 5,420 ppm/Torr, as well as the maximum higher pressure sensitivity, 500 ppm/Torr. Other design variations were also explored and the typical results are listed in Table 1. The minimum average temperature coefficient of sensitivity was -550 ppm/K.

Table 1: *Typical performance of three different sensor designs with the highest performance in each category in bold.*

Sensor Parameters	Max Low Pressure Sensitivity (ppm/Torr)	Max High Pressure Sensitivity (ppm/Torr)	Dyn. Range (Torr)	Temp. Coeff. of Sensitivity (ppm/K)
D=1 mm W=125 μm G=50 μm	5,060	380	**2,000**	-650
D=1 mm W=125 μm G=100 μm	2,170	220	1,150	**-550**
D=2 mm W=125 μm G=100 μm	**5,420**	**500**	900	-925

Sensitivity, dynamic range, and the temperature coefficient of sensitivity are metrics used to compare microdischarge-based pressure sensor designs to one another and other pressure sensors. The performance of three different sensor designs (data from two are not presented in this paper) are shown in Table 1, with the highest performance in each category in bold. The data in the table represents typical operation of each sensor design. For comparison, typical piezoresistive and capacitive pressure sensors have sensitivities of 100 ppm/Torr and 1,000 ppm/Torr respectively, and temperature coefficients of sensitivity of ±1,000 ppm/K to ± 5,000 ppm/K [12, 13].

CONCLUSIONS

The microdischarge-based pressure sensors have demonstrated an ability to operate from room temperature to 1,000˚C over the pressure range of 10-2,000 Torr. It is expected these sensors can potentially operate at temperatures below room temperature and over larger dynamic pressure ranges. They provide an electrical readout, avoiding an intermediate transduction step, which can be convenient in some cases. The active areas for these devices are small enough to permit hybrid or monolithic integration with other components that constitute functional microsystems. The sensitivity achieved compares favorably with conventional piezoresistive and capacitive pressure sensors of comparable size. The absence of a diaphragm, which is commonly used in piezoresistive and capacitive pressure sensors, also provides natural tolerance for overpressure and consequently, mechanical robustness. However, encapsulating the devices within a sealed cavity with a flexible diaphragm would permit them to be operated in a broad range of environments.

ACKNOWLEDGMENTS

This work was supported primarily by the Engineering Research Center Program of the National Science Foundation under Award No. EEC-9986866. Y. Gianchandani acknowledges support through the IR/D program while working at the National Science Foundation. The findings do not necessarily reflect the views of the NSF.

REFERENCES

[1] R. Fielder, K. Stingson-Bagby, M. Palmer, “State of the art in high-temperature fiber optic sensors,” *SPIE*, 5589(1), pp. 60-69, 2004.

[2] T. Li, Z. Wang, Q. Wang, X. Wei, B. Xu, W. Hao, F. Meng, S. Dong, “High pressure and temperature sensing for the downhole applications,” *SPIE*, 6757(1), pp. 1-7, 2007.

[3] A. Ned, R. Okojie, A. Kurtz, “6H-SiC pressure sensor operation at 600°C,” *HITEC*, Albuquerque, NM, pp. 257-260, 1998.

[4] S. Guo, H. Eriksen, K. Childress, A. Fink, M. Hoffman, “High temperature high accuracy piezoresistive pressure sensor based on smart-cut SOI,” *MEMS*, Tucson, AR, pp. 892-895, 2008.

[5] S. Fricke, A. Friedberg, T. Ziemann, E. Rose, G. Muller, D. Telitschkin, S. Ziegenhagen, H. Seidel, U. Schmidt, “High temperature (800ºC) MEMS pressure sensor development including reusable packaging for rocket engine applications,” *MNT for Aerospace Applications, CANEUS*, pp. 5p, 2006.

[6] M. Kushner, “Modeling of microdischarge devices: Plasma and gas dynamics,” *J. Phys. D: App. Phys.*, 38(11), pp. 1633-1643, 2005.

[7] C. Edelmann, “Measurement of high pressures in the vacuum range with the help of hot filament ionization gauges,” *Vacuum*, 41(7-9), pp. 2006-2008, 1990.

[8] S. Wright, Y. Gianchandani, “A harsh environment, multi- plasma microsystem with pressure sensor, gas purifier, and chemical detector, *MEMS*, Kobe, Japan, pp. 115-118, 2007.

[9] S. Wright, Y. Gianchandani, “Microdischarge-based pressure sensors for operation at 1000˚C,” *Solid-State Sensors and Actuators and Microsystems Workshop*, Hilton Head, SC, pp. 332-335, 2008.

[10] C. Wilson, Y. Gianchandani, R. Arslanbekov, V. Kolobov, A. Wendt, “Profiling and modeling of dc nitrogen microplasmas,” *J. Appl. Phys.*, 94(5), pp. 2845-2851, 2003.

[11] S. Cho, K. Najafi, C. Lowman, K. Wise, “An ultrasensitive silicon pressure-based microflow sensor,” *IEEE Trans. on Electron Devices*, 39(X) pp. 825-835, 1992.

[12] Y. Zhang, K. Wise, “Performance of nonplanar silicon diaphragms under large deflections,” *J. Microelectromech.Sys.*, 3(2) pp. 59-68, 1994.

[13] M. Gad-el-Hak, *The MEMS Handbook, Second Edition,* Boca Raton, FL, CRC Press, 2006.